

# Lamellar Crystal Orientations Biased by Crystallization Kinetics in Polymer Thin Films

Yu Ma,<sup>†</sup> Wenbing Hu,<sup>\*,†</sup> and Günter Reiter<sup>‡</sup>

Department of Polymer Science and Engineering, State Key Laboratory of Coordination Chemistry, School of Chemistry and Chemical Engineering, Nanjing University, 210093, Nanjing, China, and Institut de Chimie des Surfaces et Interfaces, CNRS-UHA, 15, rue Jean Starcky, B.P. 2488, 68057 Mulhouse Cedex, France

Received April 9, 2006; Revised Manuscript Received May 18, 2006

**ABSTRACT:** We report dynamic Monte Carlo simulations of polymer crystallization confined in thin films of thicknesses comparable to the polymer-coil sizes. We considered two contrasting affinities of the walls to the polymers, namely sticky walls that arrest the movement of polymers in contact with the substrate (such adsorbed layers allow to avoid dewetting) and slippery walls reflecting neutral repulsion of polymers. We found that at high temperatures slippery walls slightly enhance the crystallization rate with the decrease of film thickness, and the surface-assisted crystal nucleation results in dominant edge-on lamellar crystals (chain axis parallel to the wall); on the contrary, sticky walls significantly depress the crystallization rate, and the random crystal nucleation yields preferentially flat-on lamellar crystals (chain axis normal to the wall). The growth of self-seeded crystals demonstrates that the flat-on dominance is a kinetic phenomenon due to a stronger restriction on the thickening growth of edge-on lamellar crystals.

## Introduction

Thin films introduce one-dimensional spatial confinement of polymers which affects their crystallization behavior.<sup>1</sup> It is well-known that polymer crystallization is initiated by crystal nucleation, and at high temperatures, such spatial confinement will significantly lower the formation of crystal nuclei. On the other hand, flat walls may induce a preferentially parallel orientation of the conformations of the polymers in contact with these walls. This has already been identified by both diffuse neutron-scattering experiments<sup>2</sup> and molecular simulations.<sup>3–7</sup> The parallel preorientations of polymer chains can compensate to some extent for the reduction in the probability of crystal nucleation and, by the way, orient the crystals with their *c*-axis (normal to the lamella) parallel to the confining walls. Such may lead to predominantly edge-on lamellar crystals. Thus, the interaction with the walls may provide a mechanism for controlling crystal orientations and hence properties of polymer thin films.

The preferential orientations of polymer crystals in thin films have been widely studied in experiments. Roughly, experimental observations can be classified into three categories of film thickness. The first category includes those observations with films thicker than several hundred nanometers. There, predominantly edge-on lamellar crystals were found. Examples include isotactic polypropylene (iPP),<sup>8,9</sup> multilayer coextruded iPP/polystyrene (PS),<sup>10</sup> polyamide-6,<sup>11</sup> polyethylene (PE),<sup>12–14</sup> poly(ethylene oxide) (PEO),<sup>15</sup> poly(ethylene naphthalate),<sup>16</sup> poly(ethylene terephthalate) (PET),<sup>17</sup> poly( $\epsilon$ -caprolactone) (PCL) in a poly(vinyl chloride) blend,<sup>18</sup> and coarse-grained poly(vinyl alcohol) in molecular dynamics (MD) simulations.<sup>19</sup> The second category includes those observations for films of thicknesses close to the polymer coil size (<100 nm, the so-called ultrathin films<sup>1</sup>) and with the predominantly flat-on lamellar crystals. Here, examples include poly(vinylidene fluoride),<sup>20</sup> PEO,<sup>21,22</sup> PE,<sup>23,24</sup> syndiotactic PP,<sup>25</sup> iPS,<sup>26</sup> poly(3-hydroxybutyrate) (PHB),<sup>27</sup>

poly(di-*n*-hexylsilane) (PDHS),<sup>28</sup> PET,<sup>29</sup> PCL,<sup>30</sup> and a main-chain nonracemic chiral polymer.<sup>31</sup> The third category represents those observations for very thin films approaching a quasi-two-dimensional state where crystallization becomes diffusion-limited, as shown in experiments using poly(trifluoroethylene),<sup>32</sup> PEO,<sup>33–35</sup> PE,<sup>36</sup> PET,<sup>37</sup> and iPS.<sup>38</sup>

With the decrease of the film thickness, the transition from edge-on to flat-on crystals has been observed in experiments of PEO,<sup>22</sup> PDHS,<sup>28</sup> and linear low-density PE.<sup>39</sup> One might assume that this transition reflects the influence of confinement by film thickness on the formation of the critical nucleus whose size may be rather large at high temperatures. A similar transition has been observed with the increase of crystallization temperatures.<sup>40</sup> In addition, the transition from flat-on crystals to diffusion-limited aggregates has been observed with the decrease of the film thickness of PCL.<sup>30</sup> This transition reflects a competition between growth sites for polymers provided through long-distance diffusion across a depletion zone ahead of the crystal. A similar transition from flat-on faceted to branched crystals has been observed with the decrease of crystallization temperatures.<sup>38</sup>

Besides the film thickness and the crystallization temperature, the interfacial energy of the film walls also affects the preferential orientation of lamellar polymer crystals. Edge-on crystals may be selected as a consequence of epitaxial crystal growth on highly ordered walls, such as poly(di-*n*-alkylsilanes) on highly oriented pyrolytic graphite, while flat-on crystals may become dominant for high rigidity and molecular interactions to amorphous-carbon walls.<sup>41</sup>

However, up to now, the microscopic origin for the dominance of flat-on crystals in ultrathin films has not been clearly elucidated. Molecular simulations represent a powerful tool for the investigation of the underlying microscopic origin. We, therefore, launched dynamic Monte Carlo simulations to study in detail crystallization of polymers confined in ultrathin films with variable film thickness at various crystallization temperatures. We compare two extreme situations of polymer affinities to the wall, namely sticky walls with the first contact layer completely frozen and slippery walls with neutral repulsion

<sup>†</sup> Nanjing University.

<sup>‡</sup> CNRS-UHA.

\* Corresponding author. E-mail: wuhu@nju.edu.cn.

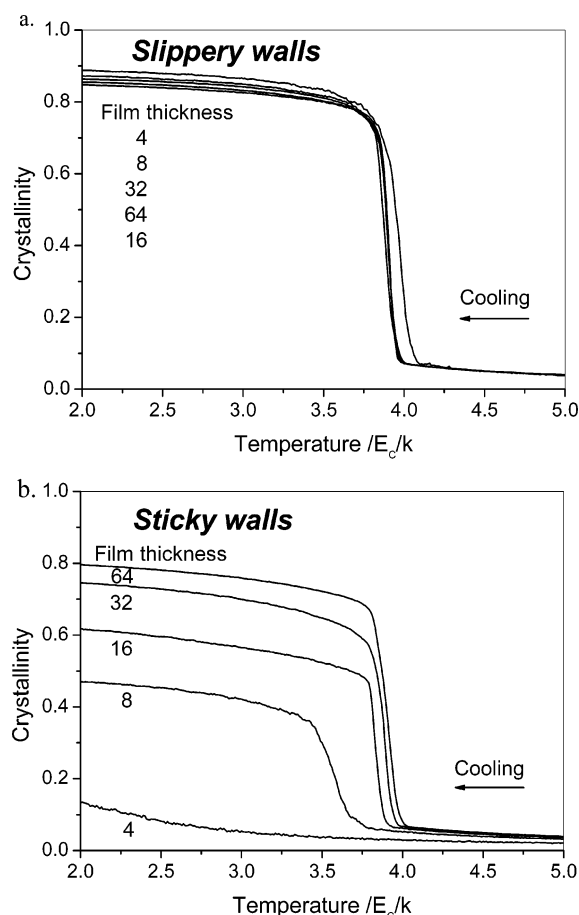


**Figure 1.** Cooling curves of crystallinity of polymer thin films with variable film thickness as denoted: (a) with slippery walls; (b) with sticky walls. The melt samples were cooled from  $5.0E_c/k$  to  $2.0E_c/k$  with the step length of 0.01 and the step period of 1000 MC cycles. The reported crystallinities represent averages over the second half of each step period.

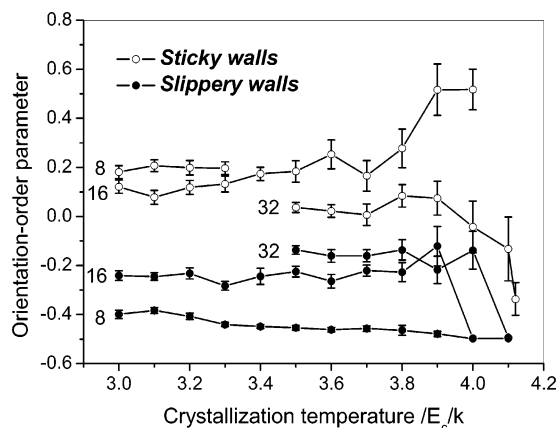


**Figure 2.** Orientation order parameter of polymer crystals after the saturated isothermal crystallization as a function of crystallization temperature for thin films of different thickness and wall affinities, as indicated. The shown data represent averages over 20 individual simulation runs based on different seeds via random-number generation. The lines are drawn to guide the eyes.

between polymers and the walls. Sticky walls can be related to the case of strong adhesion of polymers, e.g., in order to avoid dewetting, a necessary condition for the preparation of ultrathin films through spin-coating. Slippery walls can be linked to the depletion effect of polymer coils on the repulsive solid surface,<sup>42</sup> where the entropy-driven repulsion will reduce wall–polymer friction and thus enhance the mobility of polymers on the walls.

We suppose that the glass transition temperatures of ultrathin films, which has been found to decrease on repulsive walls but to increase on the highly adhesive walls,<sup>43–45</sup> may be taken as an evidence for the contrasting effects of walls with the decrease of film thickness on polymer mobility.

Our simulation results will show that, with the decrease of film thickness, sticky walls are responsible for the depression of the crystallization rate. To our surprise, we found that it is rather the reduction of the lateral crystal growth rate than due to difficulties in crystal nucleation that leads to a dominance of flat-on over edge-on crystals.

In this paper, after a short introduction to the simulation techniques, we will trace the crystallinity on cooling. Then, we will compare crystallization rates and determine the crystal orientations after the completed crystallization at variable crystallization temperatures to which the samples were quenched. After that, we perform a structural analysis of the melt as well as the isothermal crystallization process. Finally, we use a self-seeding technique to demonstrate the selection mechanism in the lateral growth of lamellar crystals of different orientations. We will present a few general conclusions at the end.

### Simulation Techniques

Dynamic Monte Carlo simulations of lattice polymers have proven to be a powerful tool for the study of polymer crystallization behaviors.<sup>46</sup> The simulations allow to move polymer chains on a lattice with microrelaxation steps. To mimic polymer thin films, we put polymer chains, each containing 128 monomers, on a  $64 \times 64 \times z$  lattice, where  $z$  is the variable film thickness ranging from 4 to 8, 16, 32, and 64 in lattice units. The film thickness is chosen as comparable to the coil sizes of 128-mers (diameters of gyration of bulk coils are about 12, a conversion from the mean-square end-to-end distances).<sup>46</sup> The lattice occupation density is kept constant at 0.9375. Periodic boundary conditions have been applied to the  $x$  and  $y$  directions, while hard walls are set at the two borders of the  $z$  direction to represent the limited film thickness. The microrelaxation steps allow the monomer to jump into its vacant neighbor, thereby changing the microconformation of polymer chains.<sup>46</sup> The time evolution of our simulations was measured in terms of Monte Carlo (MC) cycles, and each MC cycle was defined as the number of trial motions equal to the total number of lattice sites in the sample systems. The conventional Metropolis sampling algorithm has been employed for each microrelaxation step with the potential energy barrier  $\Delta E = pE_p + cE_c = (pE_p/E_c + c)E_c$ . Here, the energy parameter  $E_p$  describes the tendency for two neighboring bonds to be parallel, corresponding to the driving force for polymer crystallization, and  $p$  is the net amount of nonparallel pairs of polymer bonds, while the energy parameter  $E_c$  characterizes the conformational energy for the collinear connection of two consecutive bonds along the polymer chains, and  $c$  is the net amount of noncollinear connections. For the sake of simplicity, we set the value of  $E_p/E_c$  constant at one and change the value of  $kT/E_c$  to adjust the system temperature, where  $T$  is the temperature and  $k$  the Boltzmann constant. Under athermal conditions, we first relax the preset ordered polymer chains into the molten random coils in the thin films with fixed preset film thickness. Then, we cool the melt sample down to the variable temperatures to observe the spontaneous crystallization behaviors. We make the solid walls neutrally repulsive, corresponding to the slippery walls, while for the extremely sticky walls we reject all the trial moves involving a site of the first layer at the wall.

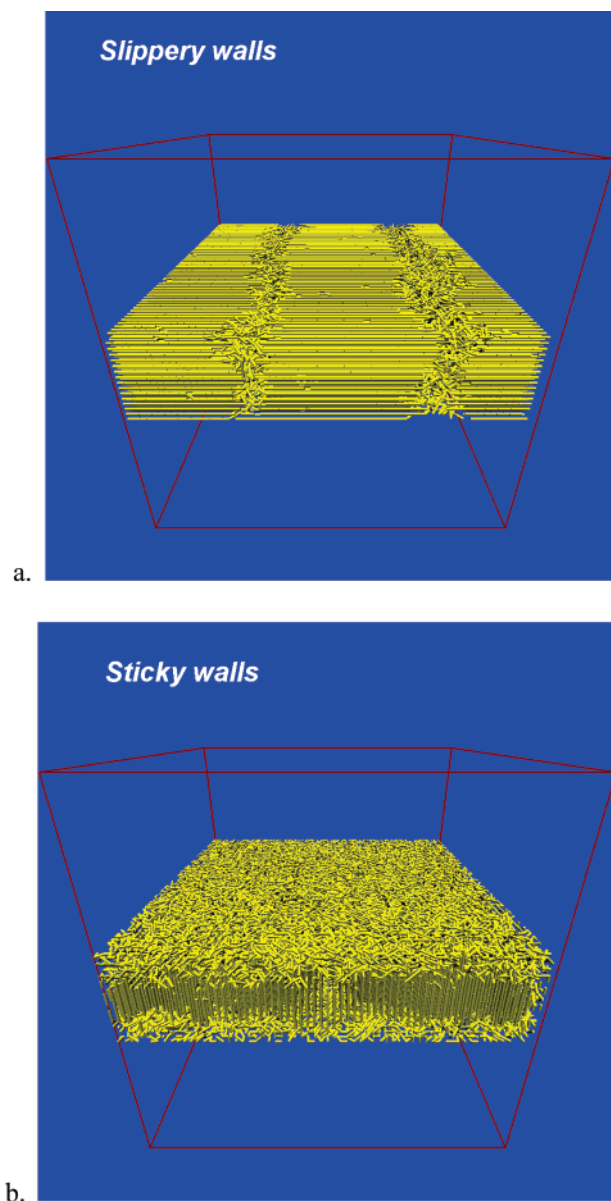


**Figure 3.** Snapshots of (a) edge-on and (b) flat-on lamellar crystals taken after the saturated isothermal crystallization at the temperature  $T = 4.0E_c/k$  for thin films of 128-mers with the film thickness 16 along the vertical direction (the other sizes of box are 64 with periodic boundary conditions) and with (a) slippery walls and (b) sticky walls. All polymer bonds are represented by cylinders.

## Results and Discussion

Under identical cooling procedures, we first compared the crystallization rates of polymer thin films with variable film thickness. To monitor crystallization, the crystallinity was defined as the fraction of bonds containing more than five parallel neighbors. The results for thin films with slippery walls and sticky walls are shown in parts a and b of Figure 1, respectively. One can see that within the same temperature region thin films with slippery walls show a weak enhancement of crystallization for the thinnest films, whereas thin films with sticky walls exhibit a significant depression of crystallization both in the rate and in the final crystallinity with decreasing film thickness. Clearly, the enhancement can be attributed to the parallel orientations of polymers near the walls, and the depression can be attributed to the restriction of polymer motions within the contact layers. Such a depression is consistent with the experimental observations on PDHS<sup>47</sup> and may also explain,

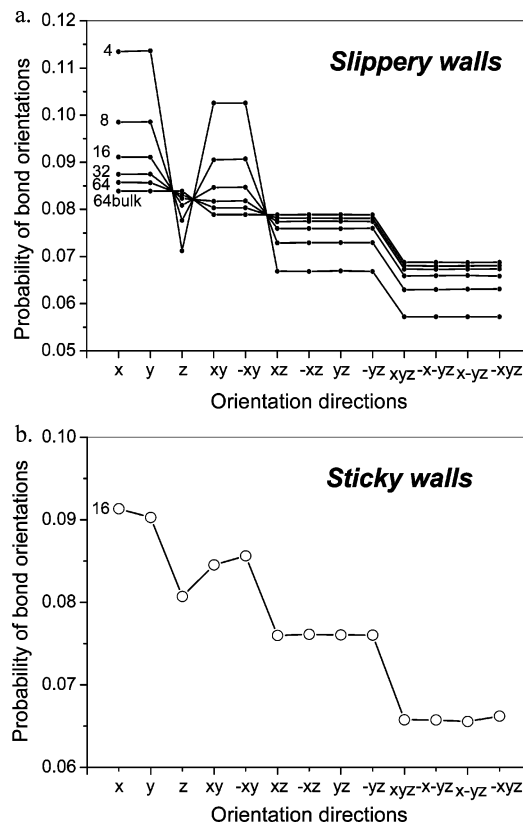


**Figure 4.** Distributions of bond orientations in the melt state of thin films with (a) slippery walls and (b) sticky walls for variable film thickness as indicated. The results are compared to the isotropic melt of bulk polymers in a  $64^3$  cubic lattice. The polymers were annealed in the melt state at a temperature of  $4.25E_c/k$  where no crystallization occurs within  $10^6$  MC cycles. From the 13 presented bond orientations, the  $x$ ,  $y$ ,  $xy$ , and  $-xy$  directions are in parallel with the plane of the thin film. The lines connecting the data points are drawn to guide the eyes.

besides the difficulty of nucleation in thin films, why amorphous ultrathin films of PHB did not exhibit crystallization at all.<sup>48</sup> In addition, a fast crystal growth rate of PET has been observed in the thin-film regions near the free surface,<sup>49</sup> while a slow crystal growth of PEO in ultrathin films has been attributed to the slowed-down diffusion of polymers near adsorbing walls.<sup>50,51</sup>

The crystal orientations obtained after completed isothermal crystallization at variable temperatures were determined for thin films of different thickness and wall affinities. To monitor the crystal orientations, the orientation order parameter was defined as  $(3\langle \cos^2 \theta \rangle - 1)/2$ , where  $\theta$  is the angle of the crystalline bonds in the statistical average with respect to the  $z$  axis, the direction normal to the plane of the film, and for all crystalline bonds which have more than five parallel neighbors. According to this definition, the orientation order parameter is expected to reach the value of one if all crystalline bonds are oriented perpendicular to the plane of the thin film, like it is the case for flat-on crystals. The orientation order parameter will get the value of  $-0.5$  if all the crystalline bonds are parallel to the film plane, like in edge-on crystals. Our simulation results are shown in Figure 2. One can see that at high temperatures thin films with the slippery walls show a dominance of edge-on lamellae, while thin films with the sticky walls show flat-on dominance at the thickness of 16 but edge-on dominance at the thickness of 32. The transition from edge-on to flat-on dominance with the decrease of film thickness is consistent with experimental observations. Thin films with sticky walls at the thickness of 8 cannot crystallize at high temperatures and thus cannot show

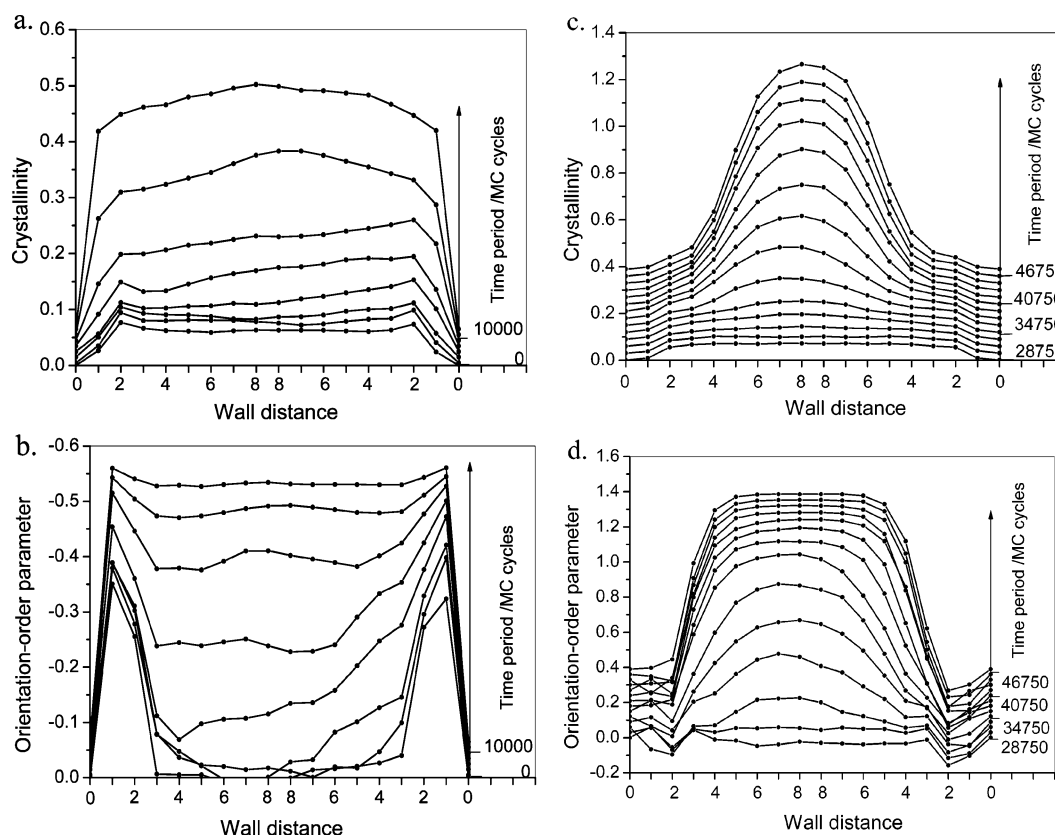


**Figure 5.** Time evolution of crystallinity (a, c) and orientation order parameter (b, d) during the isothermal crystallization of thin films with slippery walls (a, b) and sticky walls (c, d) at a temperature of  $4.0E_c/k$ . The film thickness is fixed at 16, and the curves are vertically shifted upward with the time evolution for clarity. The lines are drawn to guide the eyes.

any orientation preference of crystallites. At low temperatures, the orientation order parameter for all studied cases is close to zero, which can be attributed to random orientations of crystallites generated by the homogeneous and random crystal nucleation. Snapshots of the typical edge-on and flat-on crystals in thin films of thickness 16 are shown in parts a and b of Figure 3, respectively.

The dominance of edge-on lamellar-crystal orientations can be attributed to crystal nucleation induced by the parallel alignment of polymer coil segments in contact with the hard walls already in the melt. We may ask if for predominately flat-on lamellar crystals also a corresponding preorientation of chains in the melt exists. To find the answer, we determined the bond orientations in molten thin films for slippery and sticky walls, as shown in parts a and b of Figure 4, respectively. Indeed, for slippery walls and independent of the film thickness, polymer bonds exhibit a clear preference for parallel orientations, in agreement with experiments<sup>2</sup> and previous simulations.<sup>3–7</sup> However, also in thin films with sticky walls and for a thickness of 16, polymer bonds still prefer parallel orientations. Thus, the formation of flat-on crystals is *not* facilitated by bond orientations in the melt.

Furthermore, we traced the spatial evolution of the crystallinity as well as the orientations of the lamellar crystals (edge-on vs flat-on) during isothermal crystallization. The results are shown in Figure 5a–d. From Figure 5a,b one can see that edge-on crystals are initiated in the regions near the hard walls, given that parallel preorientations in the regions near the walls have already been existing in the melt. By contrast, in Figure 5c,d flat-on crystals start to grow in the middle region of the film away from the walls, implying a preference of the growth of flat-on crystals, although we anticipate that homogeneous nucleation will generate randomly

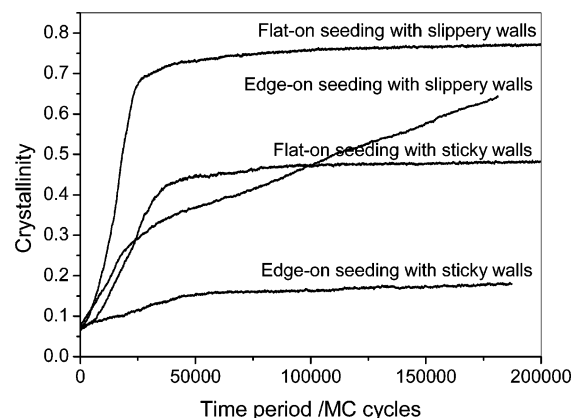


**Figure 6.** Time evolution curves of crystallinity for edge-on and flat-on crystal in thin films of thickness 16 at the temperature  $4.25E_c/k$ . The curves for thin films with slippery or sticky walls are labeled nearby.

oriented crystals in the middle region and not just flat-on crystals.

To shed light on the origin of the preference of the lamellar orientation in films, we studied the growth of crystals of two orientations initiated by the self-seeding technique.<sup>52</sup> To this end, small crystals with various well-defined orientations were spontaneously generated at temperatures slightly lower than the observation temperature. The temporal evolution of the crystallinity for edge-on- and flat-on-seeded crystals during isothermal crystallization at  $4.25E_c/k$  are shown by the curves in Figure 6. One can see that in thin films with slippery walls edge-on and flat-on crystals initially grow at the same rate. However, after this early stage, one-dimensional spatial confinement represents a significant constraint for the lateral growth of edge-on crystals,



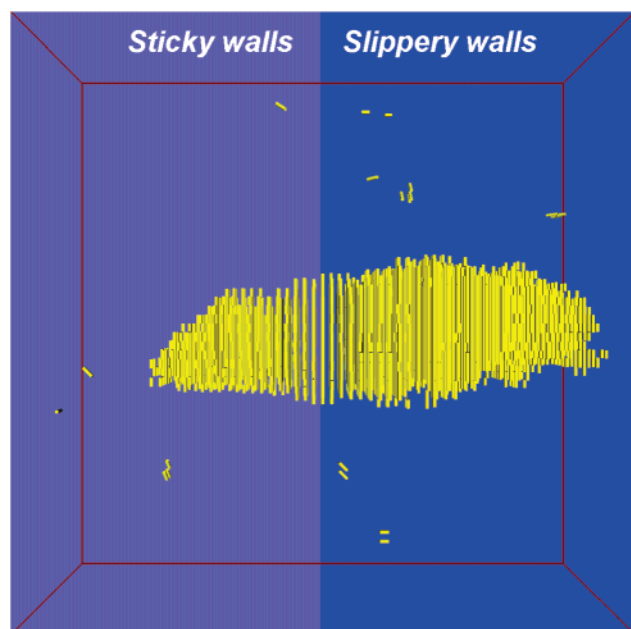


**Figure 7.** Snapshot of edge-on crystal growth in two regions with sticky wall (left half) and slippery wall (right half) separately. Only the bonds containing more than nine parallel neighbors are drawn in cylinders.

although the crystallinity can still approach eventually a high value due to thickening of the crystals. In comparison, on sticky walls, due to the strong restriction of polymer motions in the contact layers, growth of flat-on crystals is much slower and edge-on crystal growth is almost completely suppressed. Therefore, in thin films with sticky walls, flat-on crystal growth represents the dominating contribution to the final crystallinity.

The reasons for the suppression of the edge-on crystal growth is worthy to be examined further. To this end, we put an edge-on crystal at the border between two regions with contrasting wall affinities. The lateral lamellar growth into these two regions was followed. A snapshot is shown in Figure 7. One can see that on the side with the sticky wall growth of edge-on crystals is strongly hindered because of restricted thickening of the lamella at the lateral growth front. This is probably because thickening of folded-chain crystals requires a wide range of cooperation and polymer motion which is not possible or strongly hindered by the frozen contact layers for film thicknesses comparable to the coil sizes. Consequently, flat-on dominance does not occur for films thicker than about 32 because this value is beyond the coil size of 128-mers. As a matter of fact, we found that in thin films of the thickness 16 there are 16.25% of polymer coils in contact (and hence frozen) with both walls, while in thin films of the thickness 32, this fraction decreases down to 0.20%. It should be mentioned that in thin films of sticky walls the orientation of the crystals is not uniform but exhibits a strong variation at high temperatures, as indicated by the large error bars shown in Figure 2.

## Conclusions

We have investigated polymer crystallization confined in thin films by means of dynamic Monte Carlo simulations. Our results show that a decrease of film thickness leads to a slight increase of crystallization rates in thin films with slippery walls but to a significant decrease in thin films with sticky walls. At high temperatures, thin films with slippery walls exhibit dominantly edge-on lamellar crystals, while thin films with sticky walls show mainly flat-on lamellar crystals for films of thickness 16,

a value comparable to the coil size. Further structural analysis demonstrates that the edge-on dominance is dictated by crystal nucleation near the walls, while the flat-on dominance can be related to the inhibition of edge-on crystal growth mainly due to the strongly hindered thickening of crystals at the lateral growth front.

**Acknowledgment.** The research support from Nanjing University (Talent Introducing Fund No. 0205004108 and 0205004215), from the Chinese Ministry of Education (NCET-04-0448), and from the National Natural Science Foundation of China (NSFC Grant No. 20474027) is appreciated.

## References and Notes

- (1) Frank, C. W.; Rao, V.; Despotopoulou, M. M.; Pease, R. F. W.; Hinsberg, W. D.; Miller, R. D.; Rabolt, J. F. *Science* **1996**, *273*, 912.
- (2) Kraus, J.; Mueller-Buschbaum, P.; Kuhlmann, T.; Schubert, D. W.; Stamm, M. *Europhys. Lett.* **2000**, *49*, 210.
- (3) Ten Brinke, G.; Ausserre, D.; Hadzioannou, G. *J. Chem. Phys.* **1988**, *89*, 4374.
- (4) Kumar, S. K.; Vacatello, M.; Yoon, D. Y. *J. Chem. Phys.* **1988**, *89*, 5207.
- (5) Bitsanis, I.; Hadzioannou, G. *J. Chem. Phys.* **1990**, *92*, 3827.
- (6) Doruker, P.; Mattice, W. L. *Macromolecules* **1998**, *31*, 1418.
- (7) Mischler, C.; Baschnagel, J.; Binder, K. *Adv. Colloid Interface Sci.* **2001**, *94*, 197.
- (8) Padden, F. J., Jr.; Keith, H. D. *J. Appl. Phys.* **1966**, *37*, 4013.
- (9) Cho, K.; Kim, D.; Yoon, S. *Macromolecules* **2003**, *36*, 7652.
- (10) Jin, Y.; Roganova, M.; Hiltner, A.; Baer, E.; Nowacki, R.; Galeski, A.; Piorkowska, E. *J. Polym. Sci., Part B: Polym. Phys.* **2004**, *42*, 3380.
- (11) Muratoglu, O. K.; Argon, A. S.; Cohen, R. E. *Polymer* **1995**, *36*, 2143.
- (12) Hobbs, J. K.; Humphris, A. D. L.; Miles, M. J. *Macromolecules* **2001**, *34*, 5508.
- (13) Mellbring, O.; Kihlman Øiseth, S.; Krozer, A.; Lausmaa, J.; Hjerberg, T. *Macromolecules* **2001**, *34*, 7496.
- (14) Bartczak, Z.; Argon, A. S.; Cogen, R. E.; Kowalewski, T. *Polymer* **1999**, *40*, 2367.
- (15) Pearce, R.; Vancso, G. J. *Macromolecules* **1997**, *30*, 5843.
- (16) Tsuji, M.; Novillo, L. F. A.; Fujita, M.; Murakami, S.; Kohjiya, S. *J. Mater. Res.* **1999**, *14*, 251.
- (17) Durell, M.; Macdonald, J. E.; Trolley, D.; Wehrum, A.; Jukes, P. C.; Jones, R. A. L.; Walker, C. J.; Brown, S. *Europhys. Lett.* **2002**, *58*, 844.
- (18) Basire, C.; Ivanov, D. A. *Phys. Rev. Lett.* **2000**, *85*, 5587.
- (19) Baschnagel, J.; Meyer, H.; Varnik, F.; Metzger, S.; Aichele, M.; Mueller, M.; Binder, K. *Interface Sci.* **2003**, *11*, 159.
- (20) Lovinger, A. J.; Keith, H. D. *Macromolecules* **1979**, *12*, 919.
- (21) Kovacs, A. J.; Straupe, C. *Faraday Discuss.* **1979**, *68*, 225.
- (22) Schonherr, H.; Frank, C. W. *Macromolecules* **2003**, *36*, 1188.
- (23) Wittmann, J. C.; Lotz, B. *J. Polym. Sci., Polym. Phys. Ed.* **1985**, *23*, 205.
- (24) Keith, H. D.; Padden, F. J.; Lotz, B.; Wittmann, J. C. *Macromolecules* **1989**, *22*, 2230.
- (25) Bu, Z.; Yoon, Y.; Ho, R.-M.; Zhou, W.; Jangchud, I.; Eby, R. K.; Cheng, S. Z. D.; Hsieh, E. T.; Johnson, T. W.; Geerts, R. G.; Palackal, S. J.; Hawley, G. R.; Welch, M. B. *Macromolecules* **1996**, *29*, 6575.
- (26) Sutton, S. J.; Izumi, K.; Miyaji, H.; Miyamoto, Y.; Miyataishi, S. *J. Mater. Sci.* **1997**, *32*, 5621.
- (27) Abe, H.; Kikkawa, Y.; Iwata, T.; Aoki, H.; Akehata, T.; Doi, Y. *Polymer* **2000**, *41*, 867.
- (28) Hu, Z.-J.; Huang, H.-Y.; Zhang, F.-J.; Du, B.-Y.; He, T. B. *Langmuir* **2004**, *20*, 3271.
- (29) Sakai, Y.; Imai, M.; Kaji, K.; Tsuji, M. *Macromolecules* **1996**, *29*, 8830.
- (30) Mareau, V. H.; Prud'homme, R. E. *Macromolecules* **2005**, *38*, 398.
- (31) Li, C. Y.; Ge, J. J.; Bai, F.; Calhoun, B. H.; Harris, F. W.; Cheng, S. Z. D.; Chien, L.-C.; Lotz, B.; Keith, H. D. *Macromolecules* **2001**, *34*, 3634.
- (32) Lovinger, A. J.; Cais, R. E. *Macromolecules* **1984**, *17*, 1939.
- (33) Reiter, G.; Sommer, J. *Phys. Rev. Lett.* **1998**, *80*, 3771.
- (34) Reiter, G.; Sommer, J. *J. Chem. Phys.* **2000**, *112*, 4376.
- (35) Sommer, J.; Reiter, G. *J. Chem. Phys.* **2000**, *112*, 4384.
- (36) Zhang, F.; Liu, J.; Huang, H.; Du, B.; He, T. *Eur. Phys. J. E* **2002**, *8*, 289.
- (37) Sakai, Y.; Imai, M.; Kaji, K.; Tsuji, M. *J. Cryst. Growth* **1999**, *203*, 244.
- (38) Taguchi, K.; Miyaji, H.; Izumi, K.; Hoshimo, A.; Miyamoto, Y.; Kokawa, R. *Polymer* **2001**, *42*, 7443.

- (39) Wang, Y.; Ge, S.; Rafailovich, M.; Sokolov, J.; Zou, Y.; Ade, H.; Luening, J.; Lustiger, A.; Maron, G. *Macromolecules* **2004**, *37*, 3319.
- (40) Kawashima, K.; Kawano, R.; Miyagi, T.; Umemoto, S.; Okui, N. *J. Macromol. Sci., Part B: Phys.* **2003**, *B42*, 889.
- (41) Hu, Z.; Zhang, F.; Du, B.; Huang, H.; He, T. *Langmuir* **2003**, *19*, 9013.
- (42) Tuinier, R.; Taniguchi, T. *J. Phys.: Condens. Matter* **2005**, *17*, L9.
- (43) Fryer, D. S.; Nealey, P. F.; de Pablo, J. J. *Macromolecules* **2000**, *33*, 6439.
- (44) Torres, J. A.; Nealey, P. F.; dePablo, J. J. *Phys. Rev. Lett.* **2000**, *85*, 3221.
- (45) Fryer, D. S.; Peters, D. S.; Kim, E. J.; Tomaszewski, J. E.; Pablo, J. J.; Nealey, P. F.; White, C. C.; Wu, W.-L. *Macromolecules* **2001**, *34*, 5627.
- (46) Hu, W.-B.; Frenkel, D. *Adv. Polym. Sci.* **2005**, *191*, 1.
- (47) Despotopoulou, M. M.; Frank, C. W.; Miller, R. D.; Rabolt, J. F. *Macromolecules* **1995**, *28*, 6687; **1996**, *29*, 5797.
- (48) Capitan, M. J.; Rueda, D. R.; Ezquerro, T. A. *Macromolecules* **2004**, *37*, 5653.
- (49) Jukes, P. C.; Das, A.; Durell, M.; Trolley, D.; Higgins, A. M.; Geoghegan, M.; Macdonald, J. E.; Jones, R. A. L.; Brown, S.; Thompson, P. *Macromolecules* **2005**, *38*, 2315.
- (50) Dalnoki-Veress, K.; Forrest, J. A.; Massa, M. V.; Pratt, A.; Williams, A. J. *J. Polym. Sci., Part B: Polym. Phys.* **2001**, *39*, 2615.
- (51) Schonherr, H.; Frank, C. W. *Macromolecules* **2003**, *36*, 1199.
- (52) Wunderlich, B. *Macromolecular Physics*; Academic Press: New York, 1976; Vol. 2, p 52.

MA060798S